Systematic Design of Single Carrier Overlap Frequency Domain Equalization

Wladimir Bocquet, Kazunori Hayashi and Hideaki Sakai

Wladimir Bocquet is with Orange Labs Tokyo, France Telecom Japan.

Kazunori Hayashi and Hideaki Sakai are with the Graduate School of Informatics, Kyoto University.

Corresponding Author: Kazunori Hayashi

Department of Systems Science, Graduate School of Informatics, Kyoto University

Yoshida-Honmachi, Sakyo-ku, Kyoto, 606-8501, JAPAN

Tel/Fax: +81-75-753-5509 E-mail: kazunori@i.kyoto-u.ac.jp

Abstract

This paper proposes a systematic design method of overlap frequency domain equalization (FDE) for single carrier (SC) transmission without a guard interval (GI). Based on the analysis of signal-to-interference-plus-noise ratio (SINR) of the equalizer output for each symbol, we adaptively determine the block of the overlap FDE, where the block is defined as a set of symbols at the equalizer output with sufficiently low error rate, for a certain fixed sliding window size, which corresponds to a fast Fourier transform (FFT) window size. The proposed method takes advantage of the fact that the utility part of the equalized signal is localized around the center of the FFT window. In addition, we also propose to adjust the block size in order to control the computational complexity of the equalization per processed sample associating with the average bit error rate (BER) of the system. Simulation results show that the proposed scheme can achieve comparable BER performance to the conventional SC-FDE scheme with sufficient GI insertion for both the coded and uncoded cases with various modulation levels, while requiring lower computational complexity compared to the SC overlap FDE transmission with the fixed block.

Keywords- single carrier transmission, overlap frequency domain equalization, SINR

I. Introduction

Since the 90's, single carrier transmission with frequency domain equalization (SC-FDE) has been thoroughly studied and has been drawing much attention due to the effectiveness and simplicity of the transceiver [1]. When the SC-FDE is used with cyclic prefix as a guard interval (GI), the SC-FDE not only outperforms the orthogonal frequency division multiplexing (OFDM) system in the absence of channel coding, but also loosens the requirement on the power amplifiers due to the low peak to average power ratio (PAPR) of the transmitted signals. Recently, both the OFDM and the SC-FDE have been seen as complementary solutions to each other since the OFDM and the SC-FDE can coexist in a dual-mode multiple access system [2] allowing some parts of the signal processing to shift from the mobile to the base station (BS) in the uplink transmission. However, the GI is considered as a main limitation factor to achieve highly efficient signal transmission. For example, for IEEE 802.11a/g [3],[4] based transmission, the GI represents 25% of the bandwidth occupation. In order to reduce the length of the GI, the transmission with the insufficient GI insertion has been studied [5]-[7]. Moreover, some authors have proposed even no GI transmission method, which can reduce the impact of the interference caused by the absence of the GI at the cost of increased computational complexity [8]-[12]. Their solution is called overlap frequency domain equalization (overlap FDE). The basic idea of the SC overlap FDE is that, instead of adding redundancy to the transmitted signal, the head and tail parts of the FDE output, which are empirically known to be deteriorated by interference, are wasted. While the number of the FDE operations is increased, since only some portion of the FDE output is extracted as a reliable part (we call it "block" in this paper), the SC overlap FDE can achieve comparable performance to the conventional SC-FDE if the block size is small enough. In the overlap FDE, how to set the block or the block size is the key issue, because both the computational complexity and the performance largely depend on the way of setting the block, however, to the best of our knowledge, no systematic method for the determination of the block has been proposed.

In this paper, we propose a systematic design method of the overlap FDE for the SC transmissions without the GI. Based on the mathematical description of the inter-block interference (IBI) and the inter-symbol interference (ISI) for virtual vector transmission, we evaluate the SINR of each symbol at the FDE output and determine the block of the overlap FDE, so that all the symbols in the block satisfy a certain required SINR. The proposed method takes advantage of the fact that the utility part of the equalized signal is localized around the center of the FFT window. In addition, the adjustment of the block size can be also realized based on the computational complexity of the equalization per processed sample associating with the average BER. Note that the proposed design method is based on instantaneous SINR calculated by using each channel realization, therefore, the method could be worthwhile even when the statistical nature of the channel is known a priori. Simulation results show that the proposed systematic overlap FDE design scheme achieves comparable BER performance to the conventional SC-FDE scheme with sufficient GI insertion for both the coded and uncoded cases with various modulation levels. Furthermore, we highlight the complexity decrease due to the adaptive block sizing, compared to the SC overlap FDE transmission with the fixed block.

The rest of this paper is organized as follows. Section II shows the system description of the SC overlap FDE and the SINR of each FDE output is evaluated. Section III describes in detail the proposed method to determine the temporal position and the size of the block based on the SINR. Section IV presents numerical results to demonstrate the performance of the proposed method for coded and uncoded quadrature phase shift keying (QPSK) and quadrature amplitude modulation (QAM) in multipath channel environment. Finally, conclusions are drawn in Section V.

II. System Description

A. Signal Modeling and Channel Representation

The SC transmission is a traditional digital transmission scheme, in which data are transmitted as a serial stream of amplitude and/or phase modulated symbols. Let $\{x_n\}$ denote the stream of the transmitted symbols, and α_i, $i = 0, \dots, P-1$ time-invariant channel impulse response including pulse shaping filters. The received signal sequence $\{r_n\}$ can be written as

$$r_n = \sum_{i=0}^{P-1} \alpha_i x_{n-i} + e_n, \tag{1}$$

where $\{e_n\}$ is an additive white Gaussian noise (AWGN), assumed to be zero mean and independent and identically distributed (i.i.d.) with variance σ_n^2 [16].

Although the transmitted and the received signals are both serial streams in the SC overlap FDE system, we rewrite the relation between the signals using matrix and vector notation because the received signal $\{r_n\}$ is processed in a block by block manner. Defining the i-th virtual transmitted signal vector of size N as $\mathbf{x}^{(i)} = [x_0^{(i)}, \cdots, x_{N-1}^{(i)}]^T$, the corresponding received signal vector of size N, $\mathbf{r}^{(i)} = [r_0^{(i)}, \cdots, r_{N-1}^{(i)}]^T$, can be expressed as

$$\mathbf{r}^{(i)} = \mathbf{H}_0 \mathbf{x}^{(i)} + \mathbf{H}_1 \mathbf{x}^{(i-1)} + \mathbf{e}^{(i)}, \tag{2}$$

where $\mathbf{e}^{(i)} = [e_0^{(i)}, \cdots, e_{N-1}^{(i)}]^T$ denotes a corresponding AWGN vector, $\mathbf{H}_0$ and $\mathbf{H}_1$ denote the $N \times N$ channel matrices defined as

$$\mathbf{H}_0 = \begin{bmatrix} \alpha_0 & 0 & \ldots & \ldots & \ldots & 0 \\ \vdots & \ddots & \ddots & & & \vdots \\ \alpha_{P-1} & & \ddots & \ddots & & \vdots \\ 0 & \ddots & & \ddots & \ddots & \vdots \\ \vdots & \ddots & \ddots & & \ddots & 0 \\ 0 & \ldots & 0 & \alpha_{P-1} & \ldots & \alpha_0 \end{bmatrix}, \tag{3}$$

and

$$\mathbf{H}_1 = \begin{bmatrix} 0 & \ldots & 0 & \alpha_{P-1} & \ldots & \alpha_1 \\ \vdots & & & \ddots & \ddots & \vdots \\ \vdots & & & & \ddots & \alpha_{P-1} \\ \vdots & & & & & 0 \\ \vdots & & & & & \vdots \\ 0 & \ldots & \ldots & \ldots & \ldots & 0 \end{bmatrix}. \tag{4}$$

Here we define a circulant channel matrix as

$$\mathbf{H}_c = \mathbf{H}_0 + \mathbf{H}_1. \tag{5}$$

Due to the property of circulant matrices, the circulant channel matrix can be re-written as

$$\mathbf{H}_c = \mathbf{W}^H \mathbf{\Lambda} \mathbf{W}, \tag{6}$$

where $\mathbf{W}$ is a unitary DFT matrix of size $N \times N$, whose (p, q) element is $(1/\sqrt{N}) \exp(-j\frac{2\pi pq}{N})$ and $\mathbf{\Lambda}$ is the diagonal matrix representing the channel frequency response, whose diagonal elements are obtained by the DFT of the first column of $\mathbf{H}_c$. Note that, if the cyclic prefix is added as the GI before the transmission, namely for the case of the conventional SC-FDE, the received signal vector is given by

$$\mathbf{r}_{\text{cp}}^{(i)} = \mathbf{H}_c \mathbf{x}^{(i)} + \mathbf{e}^{(i)}. \tag{7}$$

B. SC Overlap FDE Receiver and Equalization

In the SC overlap FDE receiver, the same one-tap FDE as the conventional SC-FDE is firstly performed to the received signal $\mathbf{r}^{(i)}$. Since the received signal model of the conventional SC-FDE is given by (7), the FDE based on both the zero forcing (ZF) and minimum mean square error (MMSE) linear equalizers can be written by the form of $\mathbf{W}^H\mathbf{\Gamma}\mathbf{W}$, where $\mathbf{\Gamma}$ is a diagonal matrix defined as

$$\mathbf{\Gamma} = \begin{cases} (\mathbf{\Lambda}^H\mathbf{\Lambda})^{-1}\mathbf{\Lambda}^H & \text{for ZF} \\ \\ (\mathbf{\Lambda}^H\mathbf{\Lambda} + \sigma_n^2\mathbf{I}_N)^{-1}\mathbf{\Lambda}^H & \text{for MMSE,} \end{cases} \tag{8}$$

and $\mathbf{I}_N$ is the identity matrix of $N \times N$.

While for the case of conventional SC-FDE all the FDE output $\mathbf{W}^H\mathbf{\Gamma}\mathbf{W}\mathbf{r}_{\text{cp}}^{(i)}$ are used of the detection, only M $(\leq N)$ symbols of the FDE output are picked up in the SC overlap FDE receiver[12]-[15]. Denoting the extraction operation of M symbols, which corresponds to the size of block to be optimized, out of N symbols, which is the size of FFT window, by a matrix $\mathbf{V}^{N\to M}$, the FDE output after extraction, in other words, the output of the overlap FDE, can be obtained as

$$\mathbf{y}^{(i)} = \mathbf{V}^{N\to M}\mathbf{W}^H\mathbf{\Gamma}\mathbf{W}\mathbf{r}^{(i)}. \tag{9}$$

The basic procedure of the SC overlap FDE is summarized in Fig. 1. The received signal vector $\mathbf{r}^{(i)}$ is composed by windowing the received signal stream of $\{r_n\}$ with the window of width N. Then, M symbols of the FDE output are extracted to obtain the overlap FDE output $\mathbf{y}^{(i)}$. The following received signal vectors are composed by sliding the window in an overlapping manner so that the series of the extracted blocks covers the whole signal sequence.

How to determine the extraction matrix $\mathbf{V}^{N\to M}$ is the main scope of the paper and the proposed scheme will be discussed in detail in the following section. In the conventional SC overlap FDE with the fixed block[9]-[12], the selection is based on the central part of the processed sequence, therefore, for the case the extraction matrix is given by

$$\mathbf{V}_{\text{fix}}^{N\to M} = \text{diag}_N(\underbrace{0,\cdots,0}_{(N-M)/2},\underbrace{1,\cdots,1}_{M},\underbrace{0,\cdots,0}_{(N-M)/2}), \tag{10}$$

where $\text{diag}_N(.)$ is the diagonal matrix of size $N \times N$.

C. SINR Analysis of FDE Output

The output of the FDE before the extraction can be expressed as

$$\mathbf{z}^{(i)} = \mathbf{W}^H\mathbf{\Gamma}\mathbf{W}\mathbf{r}^{(i)} \tag{11}$$

Substituting Eq. (2) into Eq. (11), we obtain

$$\mathbf{z}^{(i)} = (\mathbf{W}^H\mathbf{\Gamma}\mathbf{\Lambda}\mathbf{W} - \mathbf{W}^H\mathbf{\Gamma}\mathbf{W}\mathbf{H}_1)\mathbf{x}^{(i)} + \mathbf{W}^H\mathbf{\Gamma}\mathbf{W}\mathbf{H}_1\mathbf{x}^{(i-1)} + \mathbf{W}^H\mathbf{\Gamma}\mathbf{W}\mathbf{e}^{(i)}. \tag{12}$$

By defining

$$\mathbf{\Theta} = \mathbf{W}^H \mathbf{\Gamma} \mathbf{\Lambda} \mathbf{W} - \mathbf{W}^H \mathbf{\Gamma} \mathbf{W} \mathbf{H}_1, \tag{13}$$

$$\mathbf{\Psi} = \mathbf{W}^H \mathbf{\Gamma} \mathbf{W} \mathbf{H}_1, \tag{14}$$

$$\mathbf{\Omega} = \mathbf{W}^H \mathbf{\Gamma} \mathbf{W}, \tag{15}$$

Eq.(12) can be re-written as

$$\mathbf{z}^{(i)} = \mathbf{\Theta} \mathbf{x}^{(i)} + \mathbf{\Psi} \mathbf{x}^{(i-1)} + \mathbf{\Omega} \mathbf{e}^{(i)}. \tag{16}$$

Based on the signal representation above, the SINR of the v-th element at the output of the FDE is defined by

$$\beta_v = \frac{E\Big[\left|[\mathbf{\Theta}\mathbf{x}^{(i)}]_v\right|^2\Big]}{E\Big[\left|[\mathbf{\Psi}\mathbf{x}^{(i-1)} + \mathbf{\Omega}\mathbf{e}^{(i)}]_v\right|^2\Big]}, \tag{17}$$

where $[.]_v$ and $E[.]$ respectively denote the v-th element of the vector and expectation operation with respect to the transmitted symbols and the additive noise. Assuming that the symbols and the noise are uncorrelated, the SINR can be expressed as

$$\beta_v = \frac{P_s \sum\limits_{u=0}^{N-1} |\Theta_{v,u}|^2}{P_s \sum\limits_{u=0}^{N-1} |\Psi_{v,u}|^2 + \sigma_n^2 \sum\limits_{u=0}^{N-1} |\Omega_{v,u}|^2} \tag{18}$$

where P_s is the transmit power per data symbol and $\Theta_{v,u}$, $\Psi_{v,u}$ and $\Omega_{v,u}$ are respectively the (v,u) element of $\mathbf{\Theta}$, $\mathbf{\Psi}$ and $\mathbf{\Omega}$.

For the specific case of the ZF equalization, the SINR can be further simplified as

$$\beta_v = \frac{\sum\limits_{k=0}^{N-1} \left|\frac{a_k - b_{v,k}}{a_v}\right|^2}{\sum\limits_{k=0}^{N-1} \left|\frac{b_{v,k}}{a_v}\right|^2 + \frac{\sigma_n^2}{P_s} \sum\limits_{u=0}^{N-1} |\Omega_{v,u}|^2}, \tag{19}$$

with

$$a_k = \sqrt{N} \sum_{i=0}^{P-1} \alpha_i \exp\left(-j\frac{2\pi k i}{N}\right), \tag{20}$$

and

$$b_{v,k} = \sum_{c=N-P+1}^{N-1} \sum_{k'=0}^{c-N+P-1} \alpha_{N-b+k} \cdot \exp\left(-j\frac{2\pi((v+k'))_N k}{N}\right), \tag{21}$$

where $((\cdot))_N$ denotes $\mod N$ operation. Therefore, the variation of the SINR among different symbols depends only on the value of $b_{v,k}$. When $b_{v,k}$ is close to zero, the SINR of all the symbols tend to $\frac{P_s}{\sigma_n^2}$, which means all the FDE output have the same reliability. When $b_{v,k}$ tends to the value of a_k, then the

SINR value tends to zero. In addition, the SINR can be evaluated by knowledge of the channel response and the ratio of the variance of the noise and the transmitted signal power.

III. Proposed Systematic Design of the SC Overlap FDE

We assume the availability of the channel response, the transmitted signal power and the variance of the additive noise for the evaluation of the SINR of the FDE output. Such assumption will be valid by using pilot signal with cyclic prefix as the GI. Practically, we can suppose the integration of the GI only for the pilot transmission. Let $\boldsymbol{\beta}$ denote a vector representation of the SINR as $\boldsymbol{\beta} = [\beta_0, \cdots, \beta_{N-1}]^T$. Firstly, the element of $\boldsymbol{\beta}$ with the highest SINR is identified and is denoted as β_{max}. And then, β_{max} is used as a criterion to determine the block to be optimized. To be more precise, defining ξ $(0 \leq \xi \leq 1)$ to be the acceptable SINR degradation, we set the minimum required SINR to be $\xi \cdot \beta_{\text{max}}$. Here, ξ close to 1 means that the requirement on the performance is strict, while ξ close to 0 results in low computational complexity operation. From a viewpoint of computational complexity, the block size should be as large as possible, while small size of the block is desirable from the performance point of view. Therefore, the proposed method finds the longest consecutive sequence of elements that satisfies the minimum required SINR $\xi \cdot \beta_{\text{max}}$ and determines the sequence to be the block of the overlap FDE. To be more precise, given the window size of N, the number of complex multiplications of the FDE is equal to $2N \log N + N$, since N-point FFT and IFFT operations and a multiplication of a diagonal matrix is involved. Therefore, given the block size of the overlap FDE M, the number of complex operations of the SC-FDE and the SC overlap FDE per symbol are given by $2 \log N + 1$ and $(2 \log N + 1)N/M$, respectively. In the SC overlap FDE, the factor of N/M can be considered as the penalty on the computational complexity compared with the conventional SC-FDE, while the overlap FDE does not require the GI. We can see that by increasing the size of the block M the computational complexity per symbol can be reduced. Note that the proposed approach can be easily applied to the case when the minimum required SINR is designated in different manner, such as required quality of service (QoS) defined in upper layer.

In practice, we propose to use a simple iterative process through the selected block of symbols that allows to define the longest sequence validating the constraint on the acceptable range of the SINR. It has been demonstrated in [15] via computer simulations that the effects of the ISI and ICI due to the loss of the cyclic convolution property are mainly visible at the two extreme parts of the FDE output, namely the head and tail parts of the N symbols. Fig. 2 shows typical examples of the interference power and the associated SINR based on the Eq. (19) at the FDE output with the window size of N =128 symbols. We can also see from the figure that the interferences affect the two extreme parts and that the central part of the FFT window is not degraded by the interferences. Based on the observation above, we propose a simple procedure to determine the block of the overlap FDE as shown in Table I and Fig. 3. We define M_{max} to be the index corresponding to β_{max}. Assuming that M_{max} is somewhere around the center of the window, we extend the block by moving both of its upper and lower indexes, which are respectively denoted as M_{sup} and M_{inf}, 1-by-1 from M_{max}, as far as the SINR of the extended index is greater than $\xi \cdot \beta_{\text{max}}$. Finally, the block of the overlap FDE is determined by the upper and the lower indexes.

IV. Numerical Simulation

We now evaluate the performance of the proposed method to adaptively determine the block of the overlap FDE in multi-path fading environments via computer simulations. The main simulation parameters are summarized in Table II. For the conventional SC-FDE, the equalization scheme described in [1]-[2] with (or without) appropriate GI insertion is employed. To verify the behavior of the equalization and selection method based on the SINR of each symbol at the output of the FDE, we evaluate the performance using 10-path frequency selective Rayleigh fading environment with maximum delay spread of 0.45 μs for uncoded and convolutionally coded cases. Since the system model in Table II is based on IEEE 802.11g standard [4], we have set the channel model from the system parameters of IEEE 802.11g. Throughout the simulations, we use $\zeta_{\%}$, rather than ξ, to denote the SINR degradation from β_{max}, which is defined as the percent of degradation of the SINR in dB, namely the degradation of $\zeta_{\%}$ corresponds to the SINR in dB of $(\zeta_{\%}/100) \cdot 10 \log \beta_{\text{max}}$.

A. Uncoded system

Figs. 4, 5 and 6 show the BER versus the SINR for three different modulations, namely QPSK, 16-QAM and 64-QAM, without any channel encoding scheme. The window size is set to $N =$64 and the results are presented for several values of $\zeta_{\%}$. In addition, the impact of the $\zeta_{\%}$ on the block size is also presented in Fig. 7. From all the figures, we can see that the SC overlap FDE can achieve almost the same BER performance as that of the conventional SC-FDE with the GI when the value of $\zeta_{\%}$ is large. Specifically, for the QPSK modulation, Figs. 4 and 7 show that relatively large number of the block size M is allowed for small degradation of the BER performance. For instance, for a value of $\zeta_{\%}$ equals to 80% and the window size of 64 symbols, we obtain an average block size of 40 symbols. For the case of 16-QAM or 64-QAM in Figs. 5, 6 and 7, we can see that the acceptable block size is relatively smaller than that of QPSK. This will be because of the high sensitivity to the interference due to short constellation distance for the higher modulation levels.

B. Coded System

Figs. 8, 9 and 10 illustrate the BER performances of the proposed scheme with convolutionally coded case for QPSK 16-QAM and 64-QAM, and Fig. 11 shows corresponding block size obtained by the proposed algorithm for the coded case. Again, we can see that the SC overlap FDE can achieve almost the same BER performance as that of the conventional SC-FDE with sufficient GI for small block sizes. Also, the trade off relation between the BER performance and the computational complexity, in other words, the block size, can be observed in the coded case as well. It can be concluded that the proposed method can be utilized to balance between them for both the uncoded and coded cases.

V. Conclusion

This paper proposes a systematic design of the overlap FDE for the SC transmission. Based on the analysis of the SINR of each symbol at the FDE output, an adaptive adjustment of the block of the overlap FDE, which is defined as a utility part of the FDE output, is proposed. The proposed method consists of evaluating the SINR and adjusting the upper and the lower indexes bounds of the block so as to maximize the block size for computational complexity reduction while keeping required performance. In addition, we propose to adjust the block size in order to control the computational complexity of the equalization per processed sample associating with the average BER of the system. The simulation results have validated the proposed method in terms of BER performance with QPSK and QAM modulations for uncoded and convolutionally coded cases.

In this paper, we have only used the SINR for the performance measure in the determination of the block, however, we can directly employ the BER as the performance metric by using Q-function representation[16] for the uncoded case or an approximated BER expression[17] for the coded case. Results show that the specified modulation scheme, so called SC overlap FDE could be identified as a candidate for next generation mobile communication system due to the performance and the simplicity of the scheme, especially when it is combined with systematic block design. Moreover, the proposed method could be extended to any other advanced equalization or multi-input multi output (MIMO) signal processing for the SC overlap FDE transmission and any powerful channel encoder such as the turbo codes [18] or the low density parity check codes [19]-[20].

Acknowledgment

The authors would like to thank Dr. Yukou Mochida and Mr. Jerome Laudouar of France Telecom R&D Tokyo for their valuable discussions and support.

REFERENCES

[1] H. Sari, G. Karam, and I. Jeanclaude, ”Transmission techniques for digital terrestrial TV broadcasting,” *IEEE Commun. Magazine*, vol. 33, no. 2, pp. 100–109, Feb. 1995.

[2] D. Falconer et al., ”Frequency domain equalization for single-carrier broadband wireless systems,” *IEEE Commun. Magazine*, vol. 40, no. 4, pp. 58–66, April 2002.

[3] IEEE 802.11a standard, ”ISO/IEC 8802-11”, 1999.

[4] Draft IEEE 802.11g standard, ”Further Higher Speed Physical Layer Extension in the 2.4GHz Band”, 2001.

[5] K. Hayashi and H. Sakai, ”Interference Cancellation Schemes for Single Carrier Block Transmission with Insufficient Cyclic Prefix,” *EURASIP Journal on Wireless Communications and Networking*, vol. 2008, Article ID 130747, 12 pages, 2008. doi:10.1155/2008/130747.

[6] K. Hayashi and H. Sakai, ”Per-Tone Equalization for Single Carrier Block Transmission with Insufficient Cyclic Prefix,” *IEICE Transactions on Information and Systems*, vol.E88-D, No.7, pp. 1323-1330, July 2005.

[7] D. Kim et al., ”Residual ISI Cancellation for OFDM with Applications to HDTV Broadcasting,” *IEEE Journal on Selected Areas in Communications*, vol. 16, no. 8, pp. 1590-1599, October 1998.

[8] L. Martoyo, T. Weiss, F. Capar, and F. K. Jondral, ”Low complexity CDMA downlink receiver based on frequency domain equalization,” Proc. of VTC 2003-Fall, vol. 2, pp. 987–991, Oct. 2003.

[9] W. Bocquet and M. Nakamura, ”Novel Frame Structure and Equalization Processing for ZP-OFDM Transmission,” *Proc. of WPMC 2004*, Padova, Italy, September 2004.

[10] W. Bocquet et al., ”Low Complexity Equalizer for Multi-Carrier CDMA Signal without Guard Interval,” *Proc. of ISIVC 2004*, Brest, France, July 2004.

[11] W. Bocquet et al., ”Frequency Domain Channel Equalization for OFDM system,” *Proc. of IEICE Technical Report*, RCS2003-125, Tokyo, Japan, August 2003.

[12] K. Takeda, H. Tomeba, and F. Adachi, ” Iterative Overlap FDE for DS-CDMA without GI ,” *Proc. of the 2006 IEEE 64th Vehicular Technology Conference (VTC)*, Montreal, Quebec, Canada, 25-28 Sept. 2006.

[13] H. Tomeba, K. Takeda, and F. Adachi, ” Overlap MMSE-Frequency-domain Equalization for Multi-carrier Signal Transmissions ,” *Proc. of the 9th Symposium on Wireless Personal Multimedia Communications*, pp.751-755, San Diego, USA, 17-20 Sept. 2006.

[14] H. Gacanin, S. Takaoka, and F. Adachi, ” Bit Error Rate Analysis of OFDM/TDM with Frequency-domain Equalization,” *IEICE Trans. Commun.*, Vol.E89-B, No.2, pp.509-517, Feb. 2006.

[15] K. Ishihara, Y. Takatori and S. Kubota, ”Multiuser detection using an array antenna for asynchronous single carrier systems,” *IEICE RCS*, vol. 106, no. 555, RCS2006-237, pp. 5-8, March 2007.

[16] J. Proakis, ”Digital Communications,” *3rd ed. Singapore: McGraw-Hill*, 1995.

[17] X. Qiu and K. Chawla, ”On the performance of adaptive modulation in cellular system,” *IEEE Trans. Commun.*, vol.47, no.6, pp.884–895, Jan. 1999.

[18] C. Berrou, A. Glavieux, and P. Thitimajshima, ”Near shannon limit error-correcting coding and decoding: Turbo-codes,” *Proc. of IEEE International Conference on Communications (ICC’93)*, Geneva, Switzerland, pp. 1064–1070, May 1993.

[19] R. Gallager, ”Low Density Parity Check codes,” *Cambridge, MIT press*, 1963

[20] J. Chen and M. Fossorier, ”Near Optimum Universal Belief Propagation Based Decoding of Low-Density Parity Check Codes”, *IEEE Trans. Commun.*, vol. 50, no. 3, pp.406–414, March 2002.

List of Tables

List of Figures

TABLE I

PROPOSED ALGORITHM FOR UTILITY PART SELECTION

Initialization:

Index corresponding to maximum SINR:

$M_{\text{max}} = \arg_m \max(\beta_m)$

Maximum SINR:

$\beta_{\text{max}} = \beta_{M_{\text{max}}}$

Initialization of upper and lower indexes of block:

$M_{\text{sup}} = M_{\text{max}}$

$M_{\text{inf}} = M_{\text{max}}$

Iterative process to determine upper index of block:

While ($\beta_{M_{\text{sup}}+1} \geq \xi \cdot \beta_{\text{max}}$) {

$M_{\text{sup}} = M_{\text{sup}} + 1$ (increment of upper index of block)

}

Iterative process to determine lower index of block:

While ($\beta_{M_{\text{inf}}-1} \geq \xi \cdot \beta_{\text{max}}$) {

$M_{\text{inf}} = M_{\text{inf}} - 1$ (decrement of lower index of block)

}

Final step:

Block size: $M_{\text{opt}} = M_{\text{sup}} - M_{\text{inf}}$

Extraction matrix:

$$\mathbf{V}^{N \rightarrow M} = \text{diag}_N(\underbrace{0, \cdots, 0}_{M_{\text{inf}}}, \underbrace{1, \cdots, 1}_{M_{\text{opt}}}, \underbrace{0, \cdots, 0}_{N - M_{\text{sup}}})$$

TABLE II

SIMULATION PARAMETERS

Carrier frequency	2.4 GHz
Bandwidth	20 MHz
Modulation scheme	QPSK, 16-QAM, 64-QAM
Channel encoder	uncoded or convolutionally coded
Channel estimation	Perfect CSI
Sample period	0.05μs
Number of data packets	30
Number of paths	10
Resolution of paths	0.05μs (i.e. one sample period)
Maximum delay spread	0.45μs

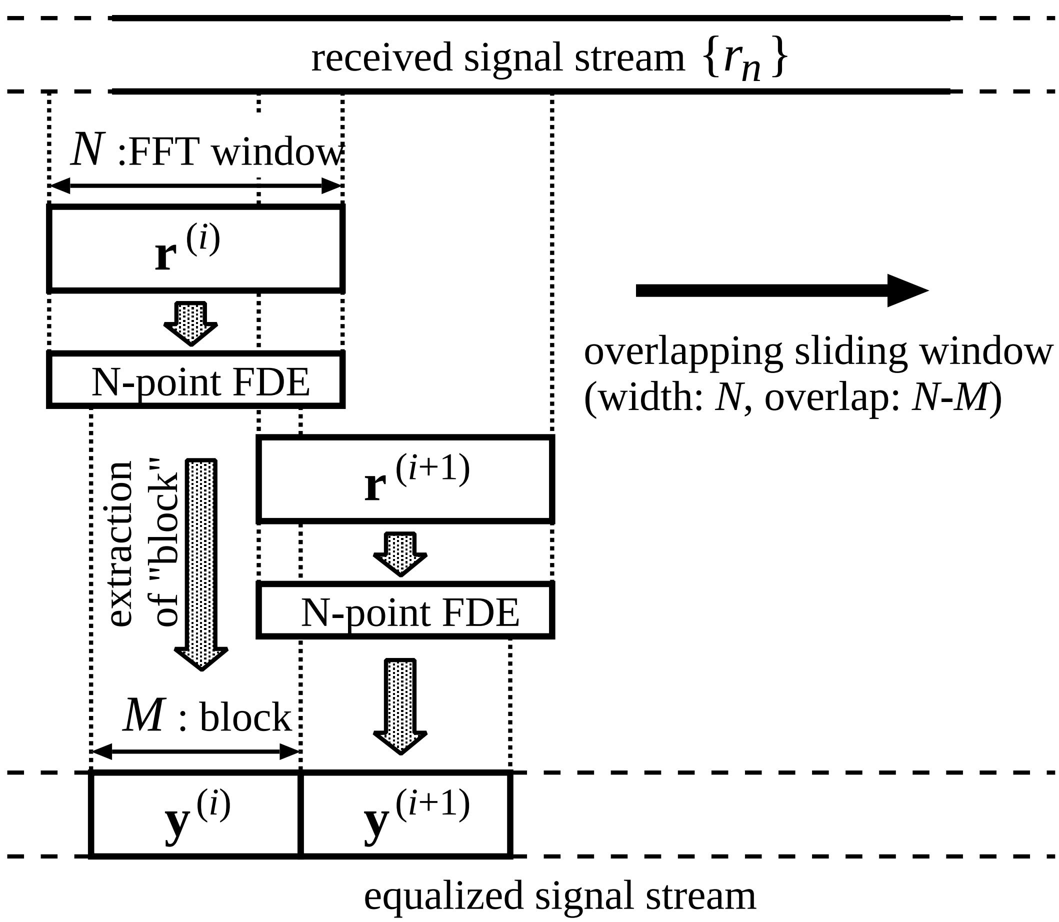

Fig. 1. Basic procedure of Overlap FDE

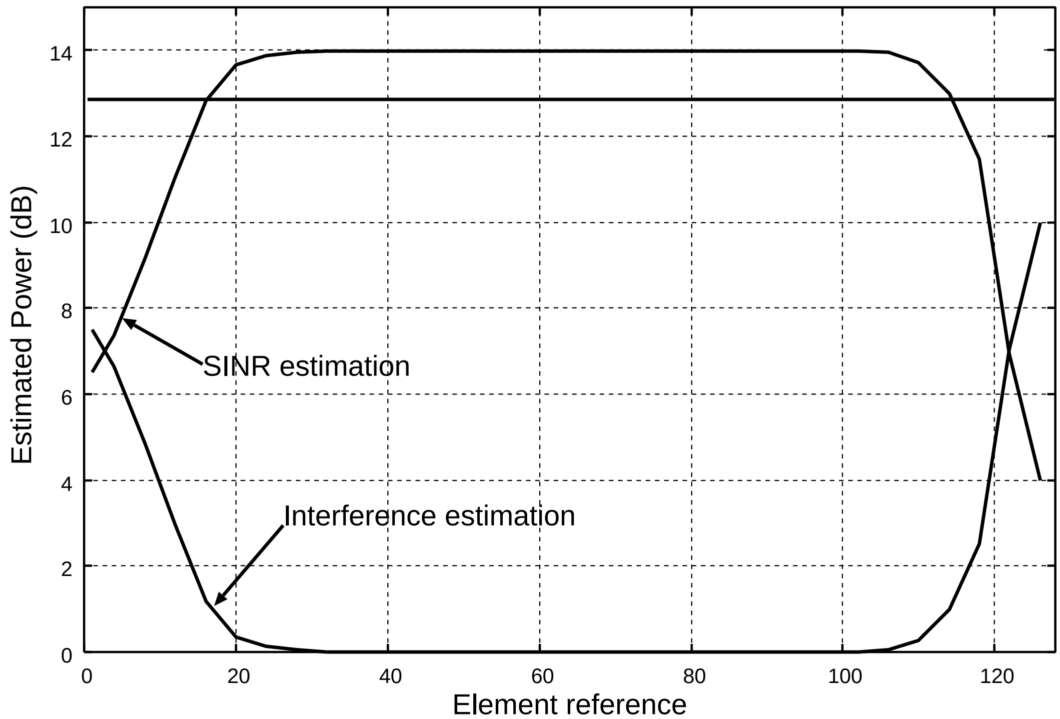

Fig. 2. Examples of SINR and Interference power for the window size $N = 128$

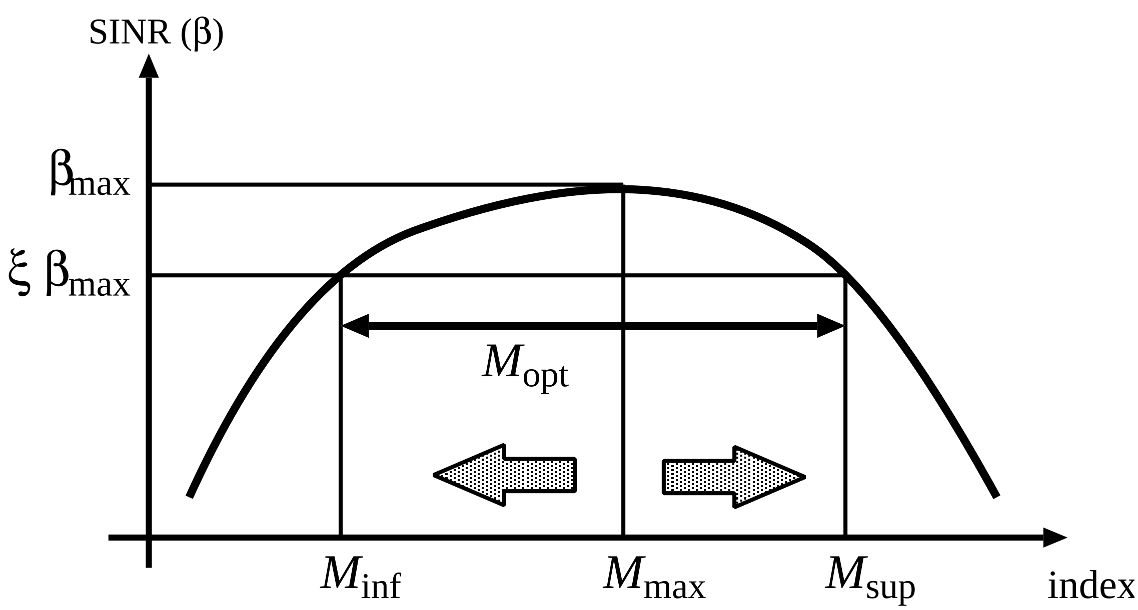

Fig. 3. M_{inf} and M_{sup} at the end of iterative process

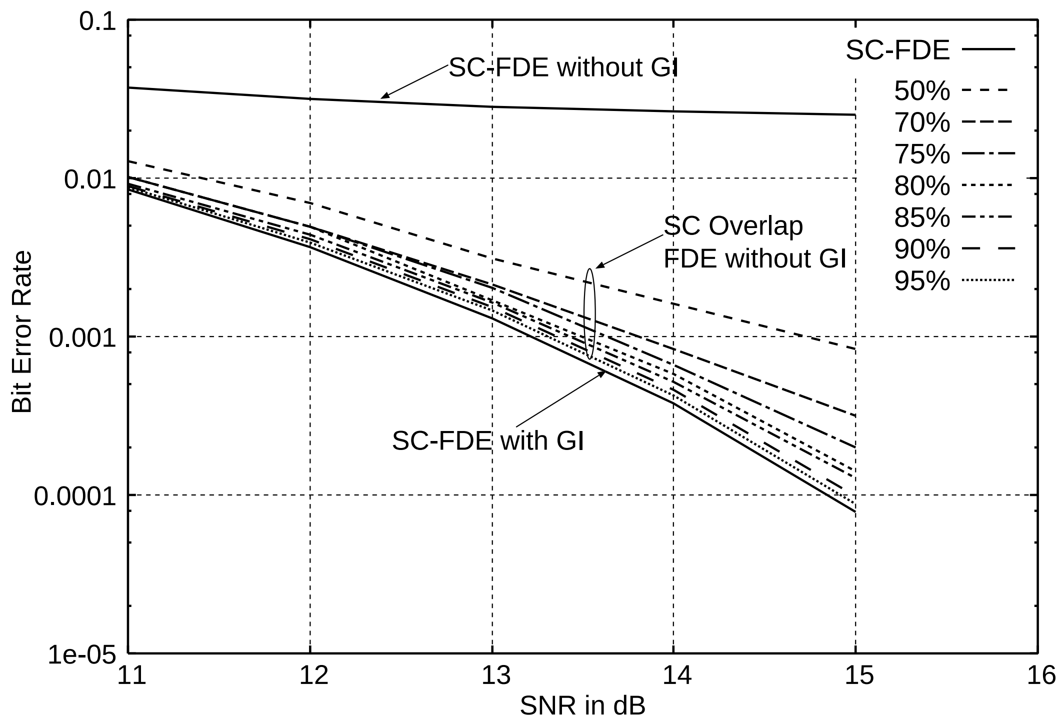

Fig. 4. BER performance for QPSK modulation, $R = 1$ and $N = 64$

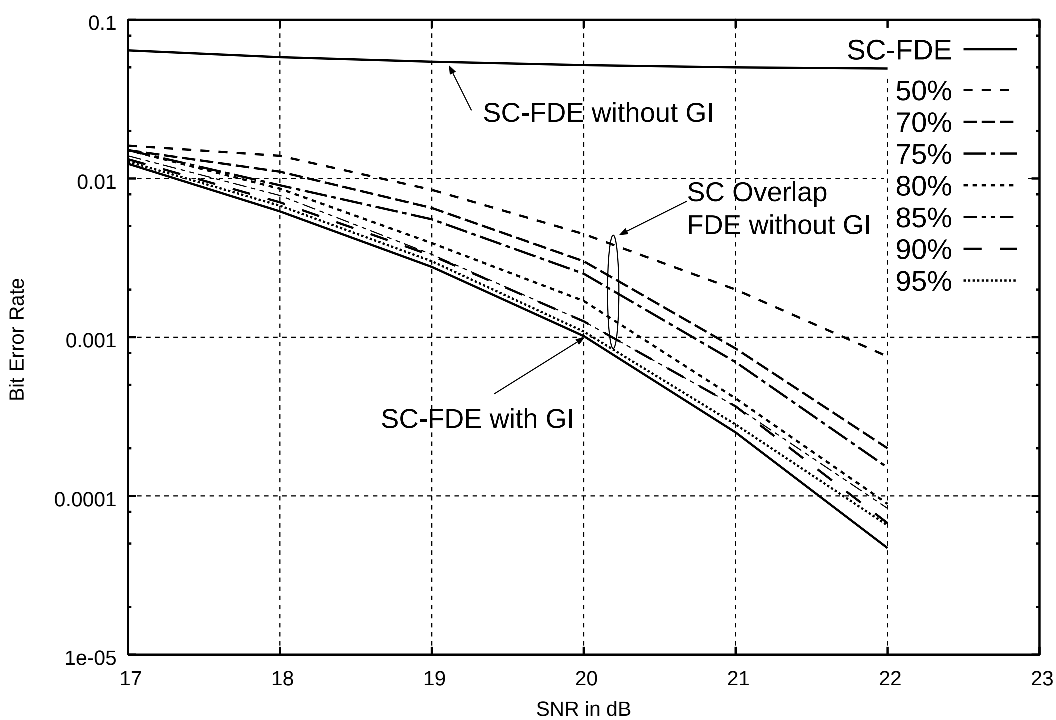

Fig. 5. BER performance for 16-QAM modulation, $R = 1$ and $N = 64$

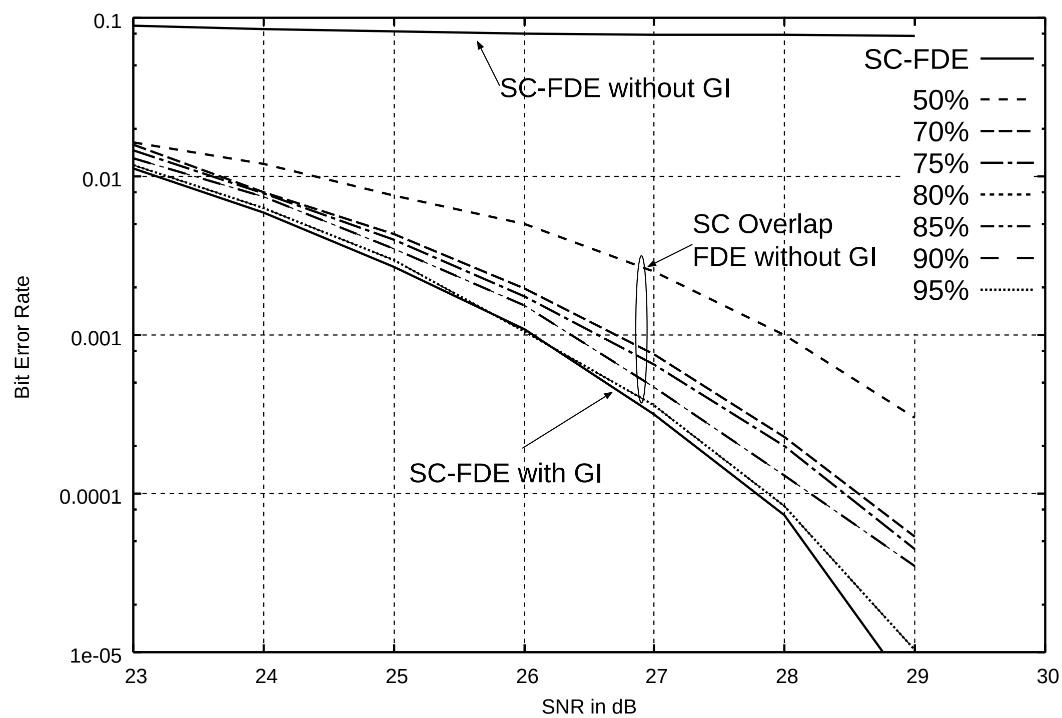

Fig. 6. BER performance for 64-QAM modulation, $R = 1$ and $N = 64$

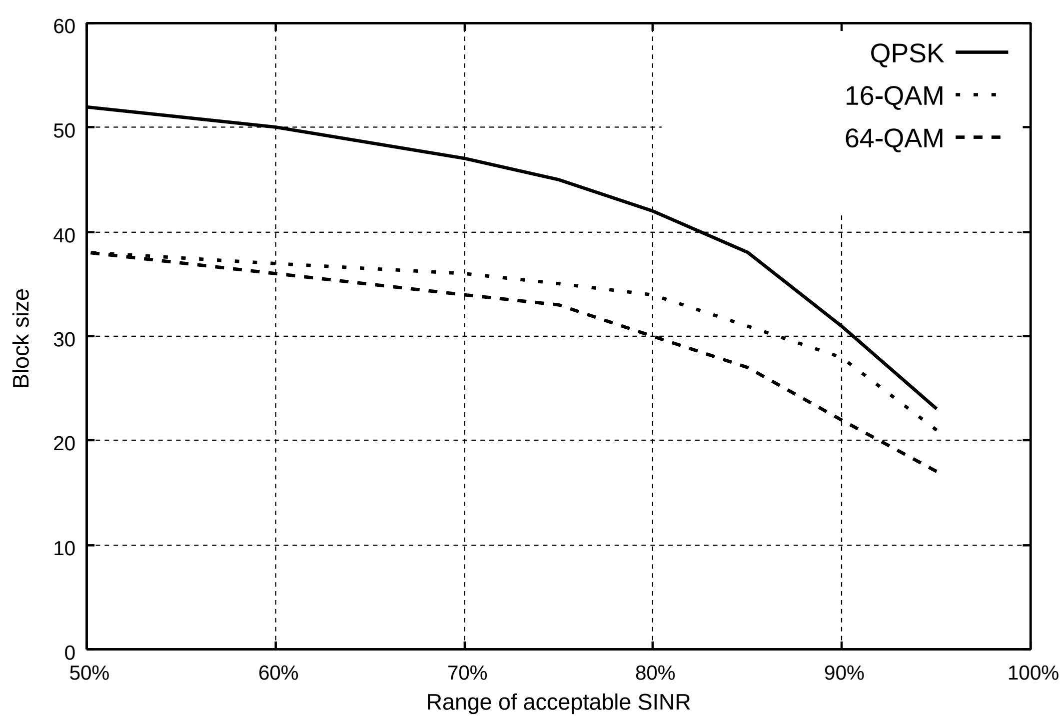

Fig. 7. Impact of SINR range on block size, $R = 1$ and $N = 64$

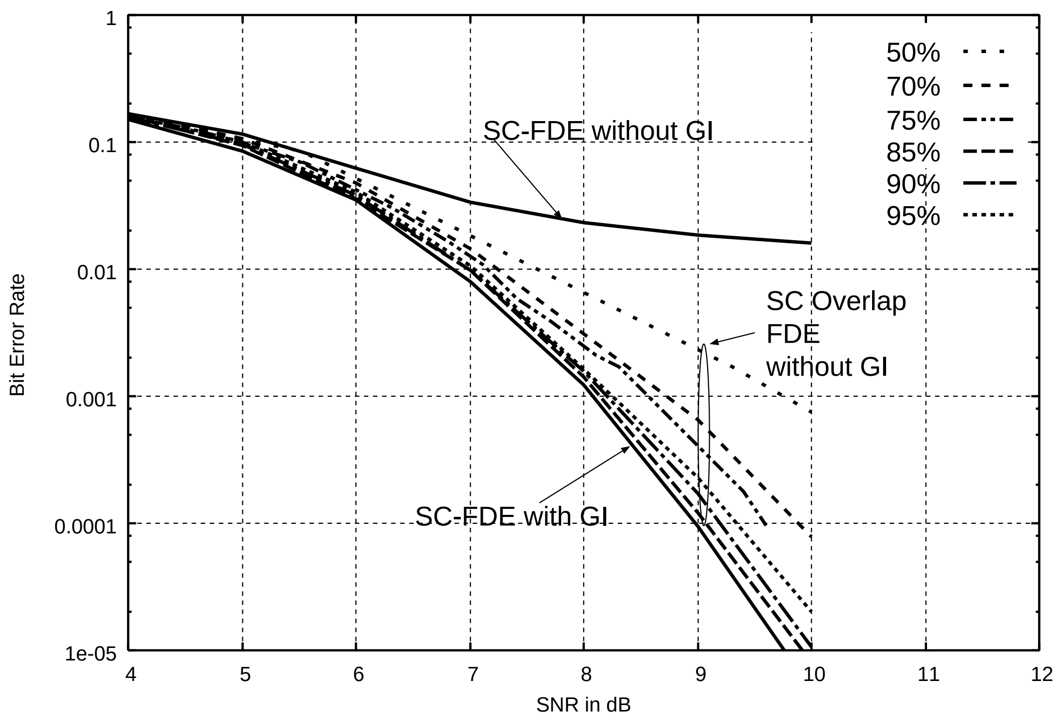

Fig. 8. BER performance for QPSK modulation, $R = 1/2$ and $N = 64$

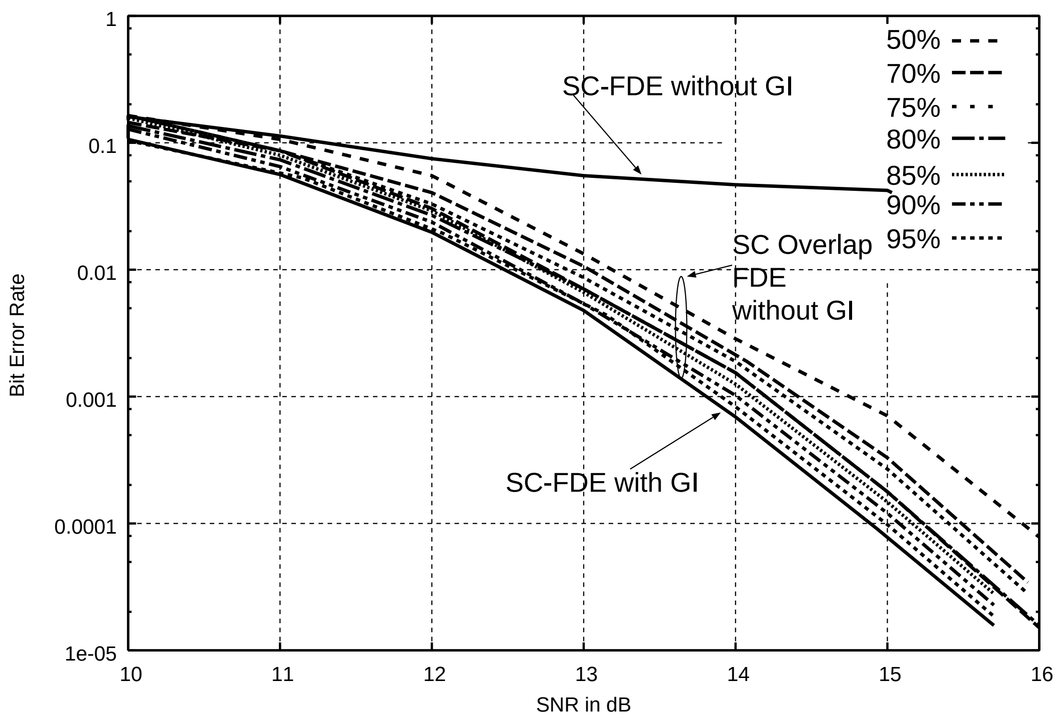

Fig. 9. BER performance for 16-QAM modulation, $R = 1/2$ and $N = 64$

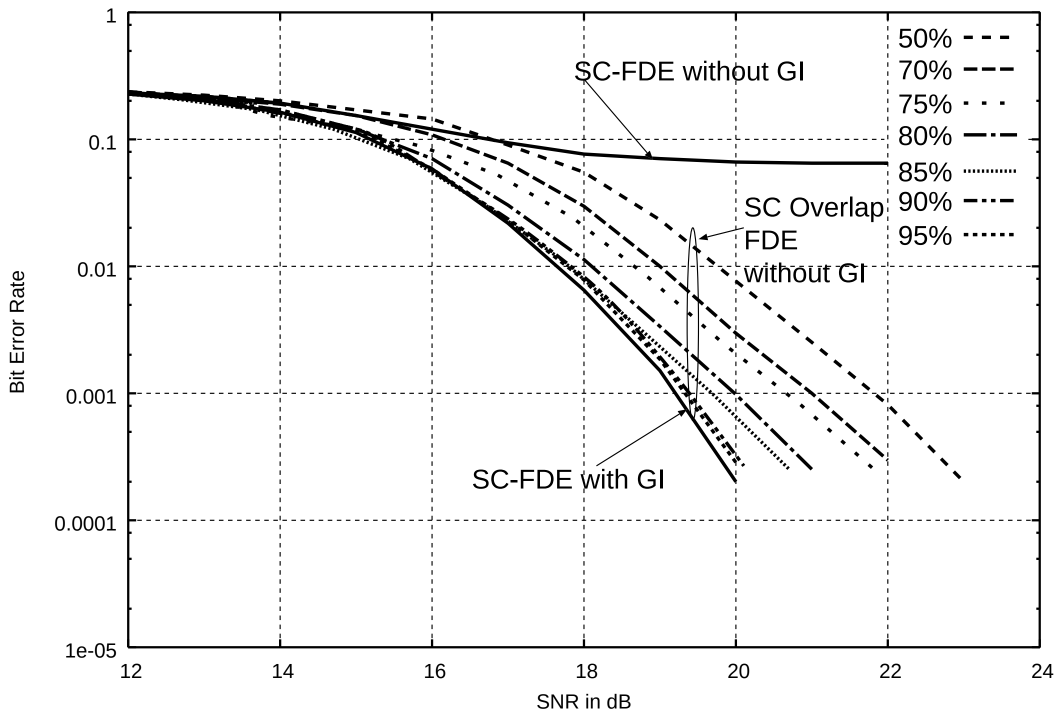

Fig. 10. BER performance for 64-QAM modulation, $R = 1/2$ and $N = 64$

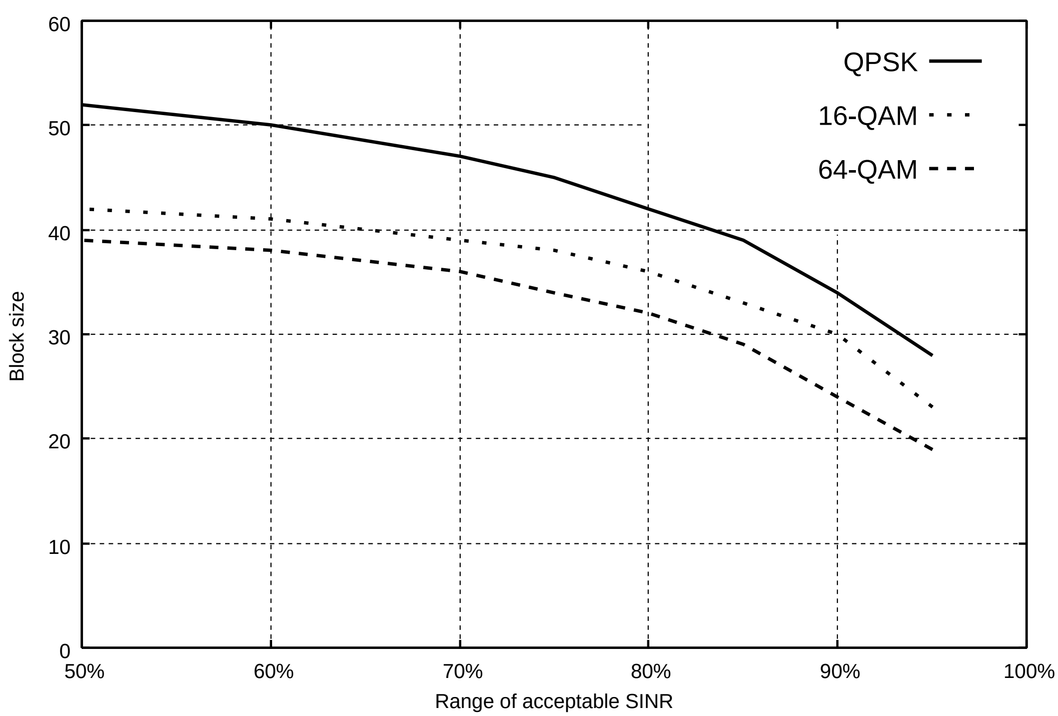

Fig. 11. Impact of SINR range on block size, $R = 1/2$ and $N = 64$